Preparation and characterization of fluorinated polypropylene by reactive extrusion with fluorinated acrylate

Si Cheng · Dijiang Wen · Guoqin Wu

Abstract The fluorinated polypropylene (PP) was prepared by reactive extrusion, in which PP was grafted with fluorinated acrylate, acrylic acid 2,2,3,3,4,4,5,5,6,6,7,7,8,8,9,9-hexadeca-fluoro-nonyl ester (HFNAE). The Fourier transformed spectroscopy results confirmed the graft polymerization on PP backbone by the reactive extrusion. The surface tension of these polymer materials and the influence of HFNAE on the crystalline behavior had been investigated with static contact angles apparatus, wide-angle X-ray diffraction (WAXD), differential scanning calorimetry (DSC) and the polarized optical microscope (POM). The surface tension of fluorinated PP was found to be less than that of the untreated polypropylene. The results showed that the fluorinated acrylate (HFNAE) might induce β form crystals when being grafted into PP from the result of WAXD and DSC. The spherule configuration difference between PP and fluorinated PP could be observed with POM photos. The result from the isothermal crystallization kinetic analyses indicated that the speed of the forming nuclear for the regular PP was smaller than that of the fluorinated PP. In addition, the addition HFNAE improved impact strength and thermal stability of PP, but the tensile tension decreased slightly.

Keywords Fluorinated acrylate · Polypropylene · Characterization · Reactive extrusion

S. Cheng · D. Wen (✉) · G. Wu
School of Materials Engineering, Suzhou University,
Ganjiang Road 178#, Suzhou,
Jiangsu 215021, China
e-mail: wendi@pub.sz.jsinfo.net

Introduction

Fluorinated polymers were paid numerous attentions due to their special performances, such as, low surface energy, low wettability, low friction and high thermal stability [1–5]. There are many physical and chemical methods to modify polymer surfaces: such as, surface fluorination directly by fluorine-gas [6–7], radical polymerization [8], copolymerization [9], plasma treatment [10]. It was reported that the fluorine treatment resulted in surfaces with low surface energy, low critical surface tension and wettability, which was close to the performance of polytetrafluoroethylene [11]. Several studies had been directed at reducing the surface tension and improving the barrier properties of polypropylene (PP) by fluorination [4]. However, surface treatment technology, such as surface fluorination directly with fluorine, was not widely used in polymer process due to the environmental and healthcare concerns.

Polypropylene is one of the commercial polymers that are widely employed in devices, automobiles and many other products owing to their advantageous properties, such as processability, mechanical properties and low cost. However, for special application, these materials are lack of necessary surface characteristics [12]. Several studies had been directed at reducing the surface tension and improving the barrier properties of polypropylene by fluorination [4]. The superior practical technique to introduce functional groups onto PP is the graft copolymerizations, which can be carried out in solution, melt phase or solid-state process on the polymer [13, 14]. The melt grafting is a preferred method due to its solvent-free condition. Melt phase reactions, so called reactive extrusion, have been studied and employed in plastic industry. Although a variety of viny and allyl monomers including

maleic anhydride [14], maleimide derivatives and maleate esters [15], glycidyl methacrylate [16], acrylic and methacrylic acid [17] have been grafted onto PP, the fluorinated acrylates have attracted much less attention.

The aim of this study was to investigate the free radical grafting of fluorinated monomers onto polypropylene in two-screw extruder, and prepared fluorinated PP with low surface tension successfully. In this study, fluorinated acrylate, acrylic acid 2,2,3,3,4,4,5,5,6,6,7,7,8,8,9,9-hexadecafluoro-nonyl ester (HFNAE), was considered. In addition, the crystalline behavior of polypropylene with and without fluorinated acrylate was analyzed by wide-angle X-ray (WAXD), differential scanning calorimetry (DSC) and polarized optical microscopy (POM). The mechanical properties of polypropylene were also been considered.

Experiment

Materials

Polypropylene (PP-2401) in powder was offered by Yanshan Petroleum Chemical company of Beijing (density=0.90~0.91 g/cm^3, MI=3 g/10 min); long carbon chain HFNAE, (liquid, B.P.=200°C; purity=96–99%; surface tension=13 mN/m), was offered by XeoGia Fluorine-Silicon Chemical company. Chemical structure of HFNAE was shown in Scheme 1. Dicumyl peroxide (DCP) was used as free radical generator, supplied by Shanghai Zhongli chemical company. Styrene (St) was be used to restrain degradation of PP and improve the grafting ratio [18, 19].

Sample preparation

The PP, DCP (0.5 wt.%), St (5 wt.%) and HFNAE were initially dry-blended and subsequently melt-mixed at a co-rotating twin-screw extruder(Φ=36 mm, L/D=40, SHJ-36, the Chenmeng company, Nanjing), at 165–190 °C and the screw speed was fixed at 70 rpm.

Characterization

Purification and characterization of grafted PP

The grafted PP samples were dissolved in refluxing xylene at a concentration of 1% (w/v) for 16 h, and then were
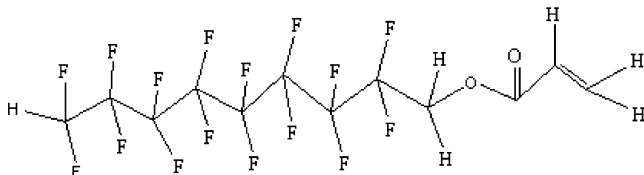
Scheme 1 The chemical structure of HFNAE

precipitated in excess acetone. The resulting polymers were filtered, washed and dried under vacuum at 80 °C for 24 h. Then the products were analyzed by Fourier transformed spectroscopy (FTIR; NICOLET 5700, American thermocorporation) with potassium bromide pellet method.

The graft ratio measurement of grafted PP

The grafted PP was dissolved in refluxing xylene and then was cooled to 70 °C. The cooled solution was added into potassium hydroxide-ethanol. A solution with a concentration of 0.03 mol/L was obtained after mixing 5 min. The graft ratio could be calculated by using the oxalic acid–ethanol solution titration.

Calculation of the surface tension

The surface tension of solid was calculation from the contact angles of the materials according to Eqs. 1 and 2, which was deduced from the surface tension component approach, advanced by Owens and Wendt [20] in 1969. The surface tension was considered to have two components, the apolar components and polar components in this approach.

$$\cos \theta = \frac{2}{r_l} \left[\left(r_l^d r_s^d \right)^{1/2} + \left(r_l^p r_s^p \right)^{1/2} \right] - 1 \tag{1}$$

$$r_s = r_s^d + r_s^p \tag{2}$$

Where γ_l denotes the surface tension of liquid–gas, γ_l^d, γ_l^p refer the apolar and polar component of this liquid, respectively. And γ_s denotes the surface tension of solid–liquid, γ_l^d, γ_l^p refer the apolar and polar component of the solid–liquid. θ is contact angle. The static contact angles were measured by JC2001-C1 static contact angles apparatus (Zhongchen technique instrument company, Shanghai, China). The value of γ_l, γ_l^d and γ_l^p of water and ethylene glycol at 20 °C are listed in the Table 1.

Wide-angle X-ray diffraction

Wide-angle X-ray diffraction was conducted on a PW1700 X-ray diffractometer. Graphite monochromatic Cu Kα radiation was employed as a radiation source.

DSC analysis

The melting behavior of PP and grafted PP were carried out using a Perkin–Elmer Diamond differential scanning calorimeter under nitrogen. Samples were heated from 50 to 200 °C with a rate of 10 °C/min and kept the temperature at 200 °C for 5 min afterwards. Then the system was cooled from 200 to

Surface tension and components of water and ethylene glycol (20 °C)

Probe liquid	Surface tension(mN/m)		
	γ_l	γ_l^d	γ_l^p
Water	72.8	21.8	51
Ethylene glycol	48	29	19

50 °C with a rate for 10 °C/min. Subsequently, the samples were heated again from 50 to 200 °C with a rate of 10 °C/min.

Polarized optical microscopy

The isothermal crystallization process of PP and fluorinated PP in thin film, at the temperature of 125 °C were studied with optical microscopy, according to the same procedure used to study the isothermal crystallization process of the PP phase. Polarized optical microscopy fitted with the hot stage was used. Optical micrographs were taken with crossed polarizer.

Isothermal crystallization kinetic studies of PP were conducted by using optical depolarization instrument (GJY-III, the material institute of Donghua University, Shanghai, China).

Melt index measurement

Melt index was carried out with melt index measuring apparatus (RL-11B, Shanghai S.R.D scientific instrument CO., LTD), according to ASTMD1238-95.

Mechanical properties

Tensile testing was carried out according to ASTM 638-03: standard test method for tensile properties of plastics using WST-II universal tester (from Shenzhen Kaiqiangli Testing Instruments Co., Ltd.).

Izod impact strength with notch was carried out according to ASTM D256-06 using izod impact test machine (XJU-22,Chengde Precision testing machine Co., Ltd)

Thermal deformation temperature was carried out according to ASTM D 648-06 by using Heating Deflection and Vicat Softening Temperature Measuring Apparatus(RV-300E, Chengde Precision testing machine Co., Ltd)

Results and discussion

FTIR analyses

Figure 1 showed the FTIR spectra of HFNAE, the absorption at the 1,739.0 cm^{-1} could be attributed to the stretching vibration of carbonyl group(C=O), and the peaks
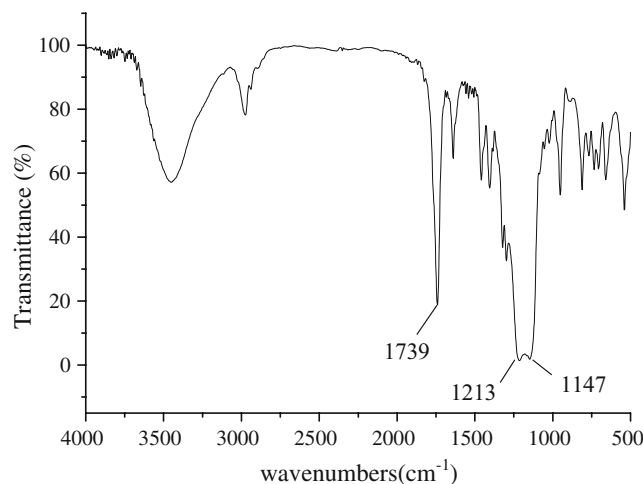
Fig. 1 The FTIR spectra of HFNAE

at 1,213 and 1,147 cm^{-1} be attributed to the stretching vibrations of –CF$_2$, respectively. In the FTIR spectra of fluorinated PP, these typical stretching vibration bands, such as 1,727 cm for carbonyl group, 1,209 and 1,151 cm^{-1} for –CF$_2$ group, were still present, seen Fig. 2.

Table 2 showed the graft ratio of fluorinated PP. From the Table 2, it could be found that the graft ratio of fluorinated PP reached to 7.2% when the content of HFPMA was increased to 20 wt.%.

Surface wettability

The surface tensions of the materials were calculated according to Eqs. 1 and 2, were shown in Fig. 3. It was found that PP had a lower surface tension after grafting with HFPMA. The surface tension decreased more quickly at low fluorine content than at high content, and then went to steady. The surface tension reached 18.7 mN·m^{-1} when in a PP containing 20% (by weight) of HFPMA due to the lower surface tension value of HFNAE (=13 mN/m).
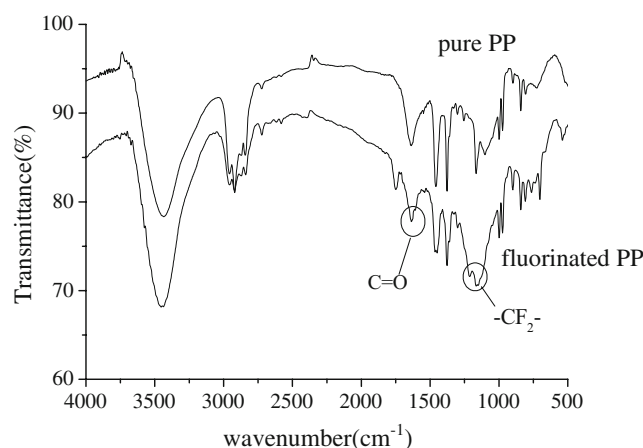

Fig. 2 The FTIR spectra of pure PP and fluorinated PP (the content of HFNAE=20 wt.%)

Table 2 The graft ratio of grafted PPs

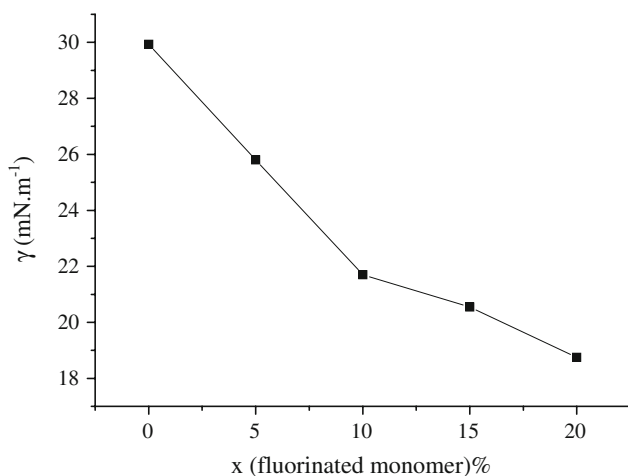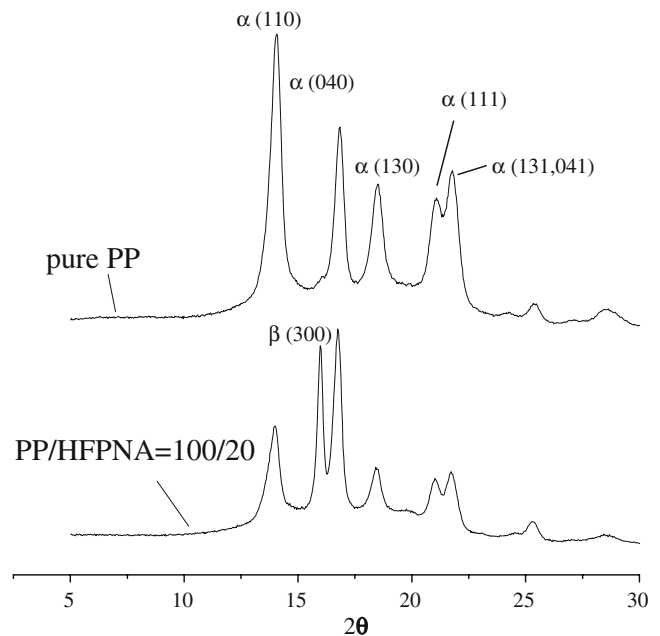| Sample	PP0	PP5	PP10	PP15	PP20
PP/HFPMA	100/0	100/5	100/10	100/15	100/20
Graft degree (%)	0	1.4	3.3	5.8	7.2

X-ray diffraction analyses

The X-ray diffraction (XRD) spectra of pure PP and fluorinated PP were shown in Fig. 4 and the assignment of the crystal plane to the different diffraction peaks was also shown. The four main diffraction peaks of PP were at 2θ equal to 13.97°, 16.74°, 18.49°, 21.03° and 21.72°, as (110), (040), (130), (111) and (041, 131) crystal plane respectively, which are the typical α-form monoclinic structure of PP. The main diffraction angle of β-form hexagonal structure was at 15.98° as (300) crystal plane [21]. Therefore, conclusion could be made that, the (300) crystal plane that was assigned to β-form emerged after grafting, and it indicated that the fluorinated PP had emerged mixed crystal structure-the α-form co-existed with β-form.

All the curves through deconvolution auto fitting peaks with Gaussian Function and the crystallinity of α- and β-forms were calculated and listed in Table 3. The data showed that the crystallinity decreased while the relative content of β form crystal, K_β (%), reached 20.8% in a PP containing 20% (by weight) of HFNMA.

DSC analyses

The DSC heating and cooling curves of PP and fluorinated PP were shown in the Fig. 5. As shown in Fig. 5, the fluorinated samples had two melting peaks at the second heating cycle which centered at 165.6 and 150.2 °C after removing the history effect. The peak at 165.6 °C could be

Fig. 4 The XRD curve of pure PP and fluorinated PP

attributed to the melting of the α-crystals, and the peak at 150.2 °C could be attributed to the melting of the β-crystals [22, 23]. In addition, the crystalline temperature increased after grafting HFNMA, from 114.5 to 116.8 °C slightly due to β-crystals existence [24].

The percentage of β phase of a sample, Φ_β, was determined by the relative crystallinity of α phase and β phase:

$$\Phi_\beta = \left[X_\beta / \left(X_\alpha + X_\beta \right) \right] \times 100\% \tag{3}$$

Where, X_α and X_β are the crystallinity of the α phase and β phase, respectively. Because of the coexistence of α phase and β phase crystals in the samples, the crystallinity of the α phase and β phase were calculated separately according to equation:

$$X_i = \Delta H_i / \Delta H_i^0 \times 100\% \tag{4}$$

Where ΔH_i is the fusion heat of either the α phase and β phase, and ΔH_i^0 is the standard fusion heat of either α phase, 178 J/g [25], or β phase crystals, 170 J/g. [25]

The results are listed in Table 4. Depending on the Eqs. 3 and 4, after grafting G06D, the crystallinity of α phase and β phase were calculated to be 29.2% and 5.8%

Fig. 3 Effect of the content of HFPNA on surface tension of PPs

Table 3 The crystallinity and crystalline dimension of PP0 and fluorinated PP (PP20)

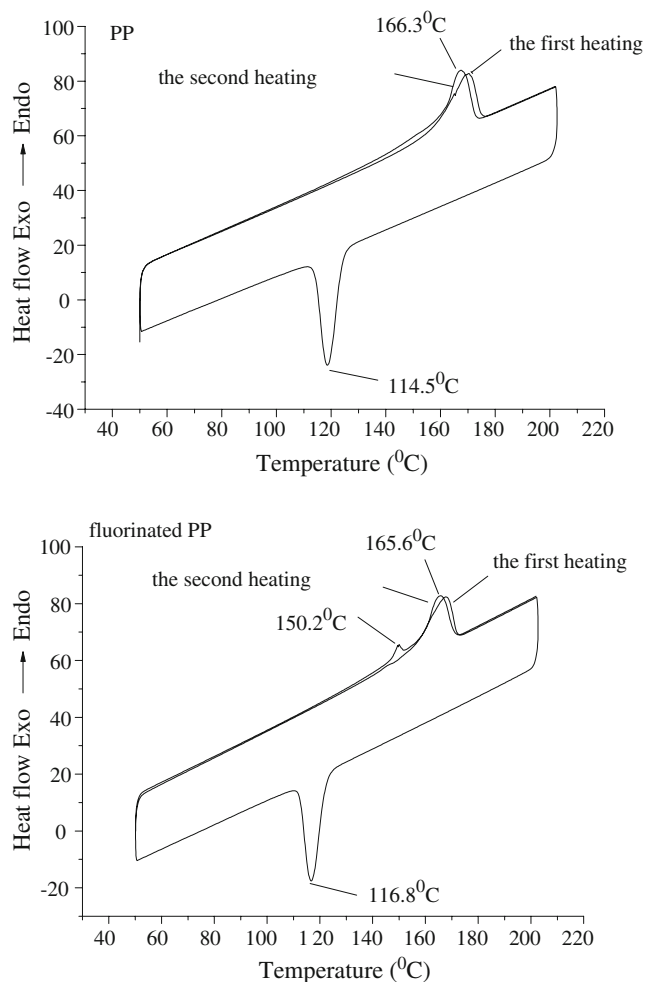| Sample		PP0	PP20
Degree of crystallinity	Xc α	79.4	69.5
	Xc $\alpha+\beta$	79.4	71.6
Relative content of β-crystal	K_β (%)	–	20.8

Fig. 5 The DSC curve of pure PP and fluorinated PP (PP20)

POM analyses

Figure 4 showed the spherulite grow at isothermal crystal growth process of pure PP and fluorinated PP. The spherulite matting ring was also observed in the Fig. 6. The images showed that there were some differences between the pure PP and the fluorinated PP. The spherulites in fluorinated PP were much blurrier than that in pure PP. In addition, there were some screw striations at the edge of spherulites. The β form lamellar crystals exhibit neither the peculiar lath-like form nor the crosshatched lamellar morphology while are consistently observed to show an extended sheet morphology characterized by frequent giant screw dislocations [26–29].

The spherulite size of the pure PP (diameter=90 μm) was smaller than that of the fluorinated iPP (diameter= 110 μm), the nucleus-forming rate of PP (about 11/60 s) was more rapid than that of the grafted PP (about 7/60 s). In addition, it became more difficult to distinguish the borders between the different spherulites in fluorinated PP

Isothermal crystallization kinetic analyses

The Avrami formula often can be used to study the polymer isothermal crystallization kinetic. The Avrami can be shown as fellows:

$$\lg\left(\ln\frac{I_\infty - I_0}{I_\infty - I_t}\right) = \lg K + n\lg t \qquad (5)$$

From previous DSC curves (Fig. 5), it could be found that the crystalline temperature of PP and fluorinated PP were 114.5 and 116.8 °C respectively. So, the isothermal crystalline temperature in isothermal crystallization process was chose at 113, 115 and 119 °C.

The plot of $\lg(\ln((I_\infty - I_0)/(I_\infty - I_t)))$ versus lgt for isothermal crystallization can be depicted as in Fig. 6 depending on the result of the optical depolarization instrument. Through the linear fitting ($Y = A + B \times X$), the crystallization rate constant, K, and the Avrami index, n, can be calculated and listed in Table 5.

Figure 7 displayed the isothermal crystallization Avrami curves. It can be found that, at different temperatures, the crystallization rate constant apparently decreased after polypropylene grafting fluorinated acrylate. It meant the crystallization rate was slower after grafted HFNMA.

The reason may be that there are many C–F groups at the HFNAE outer-layer, and fluorinate groups block PP main chain movement. So the PP molecules move more slowly between the melt and crystal interface, and at fixed time period, the number of forming crystal nucleus decreased, the crystallization rate decreased too.

Mechanical properties

Table 6 showed the melt index of PP0 and grafted PPs. It could be seen that the melt index decreased slightly from 9.2 g/10 min to 6.5 g/10 min after grafting HFNAE. It was because that the side chain lengthened after grafting HFNAE. The fluorinated long side chain blocked the segment moving, so the flowability of fluorinated PP descended, the same as melt index.

Table 4 The crystallinity of α phase and β phase from DSC

Sample	α-melting point (°C)	β-melting point (°C)	ΔH_α(J/g)	ΔH_β(J/g)	X_α(%)	X_β(%)	X (%)	Φ_β(%)
PP0	166.3	–	68.58	–	38.5	–	38.5	–
PP20	165.6	150.2	49.03	2.8	27.5	1.7	29.2	5.8

Fig. 6 Polarizing micro-
scope photos of PP at the cool-
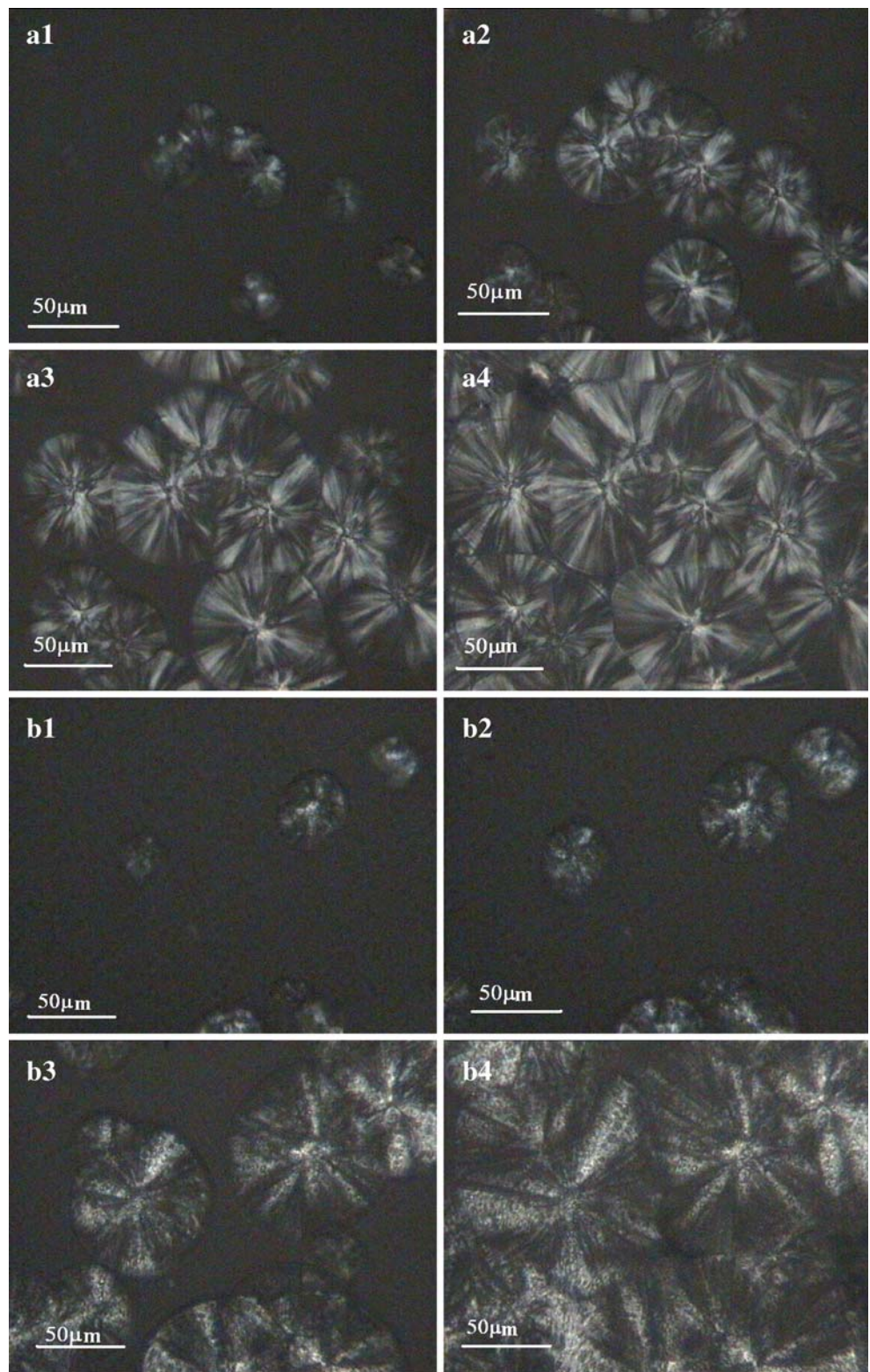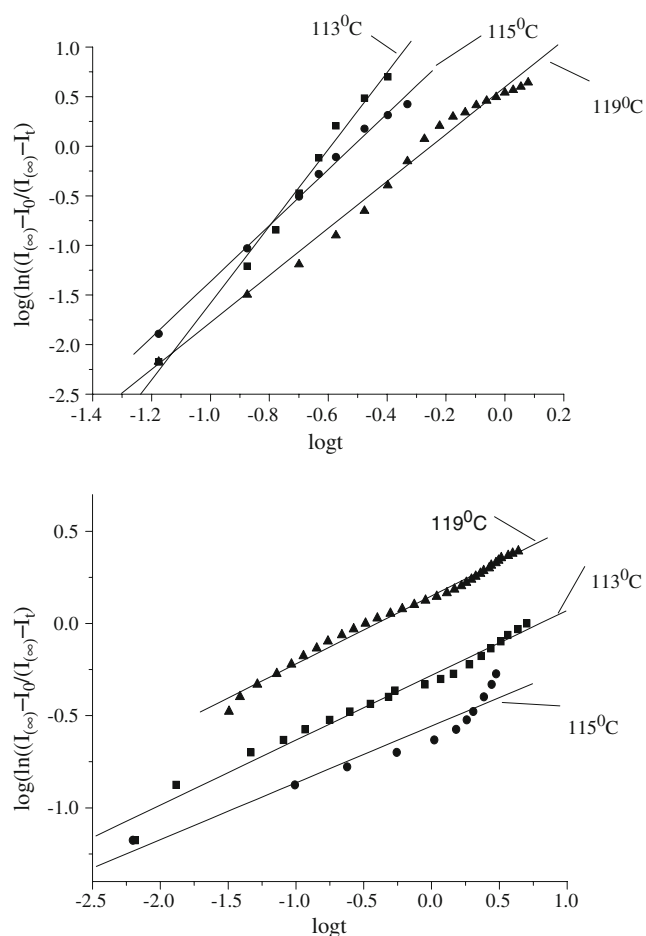ing crystallization process (*a1–
a4*) PP0; (*b1–b4*) PP15 (interval
30 s)

Table 5 Avrami equation parameter at isothermal crystallization

	113 °C		115 °C		119 °C	
	K	n	K	n	K	n
PP0	195	3.88	28.8	2.82	3.8	2.37
Fluorinated PP (PP20)	0.52	0.35	0.28	0.31	1.41	0.37

Table 6 The melt index of PP0 and grafted PPs

Sample	PP0	PP15	PP20
PP/HFPMA	100/5	100/15	100/20
Melt index (g/10 min)	9.2	7.3	6.5

The mechanical test results of PP and fluorinated PP were shown in Fig. 8. It could be seen that tensile strength decreased slightly with the content of HFNAE increasing. This might be the result of reduction of crystallinity of fluorinated PP.

Table 7 showed the room temperature notched Izod impact strength and thermal deformation temperature of PP and fluorinated PP. It can be seen that the impact strength of PP increased from 3.3 to 5.5 KJ/m^2 due to the β crystal existence after grafting HFNAE [24]. It also could be found

that the thermal deformation temperature of fluorinated PP increased from 128 to 135 °C due to C–F bond existence. It was well-known that the C–F bond was super stable because there exited some extent overlaps between 2s-orbital, 2p-orbital of fluorine atom and corresponding orbital of carbon atom [1].

Conclusion

The study revealed that HFNAE was successfully incorporated onto PP backbone by reactive extrusion. HFNAE which be grafted onto polypropylene could induce β form crystal depending on the result of WAXD and DSC and decreased the surface tension of PP. After grafting HFNAE, there are many C–F groups at PP side chain, fluorinated groups block PP main chain movement, destroy the crystallite regularity at the crystal growth process, and the crystallization rate reduced. In addition, the tensile strength of fluorinated PP decreased owing to the devaluation of crystallinity. In the polarized micrographs of fluorinated PP, there are some screw striations in the edge of spherulites. In addition, the addition fluorinated methyacrylate improved impact strength and thermal stability of PP, respectively from 3.3 to 5.5 KJ/m^2 and from 128 to 135 °C, but the tensile strength decreased slightly.

Fig. 7 Isothermal crystallization Avrami curve at different temperature
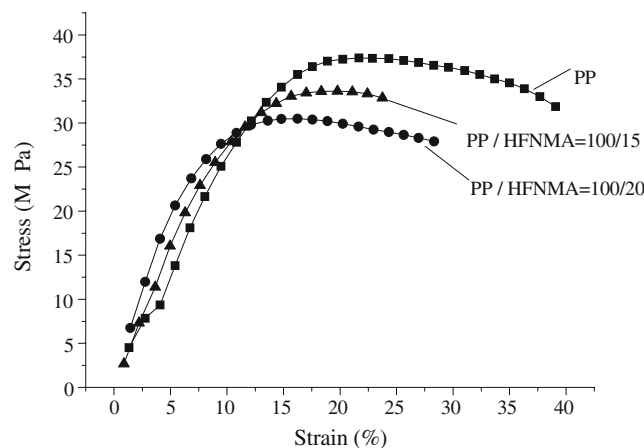

Fig. 8 The tensile stress-strain curve of PP and fluorinated PP

Table 7 Izod impact strength and thermal deformation temperature of PP and fluorinated PP

	Impact strength (KJ/m^2)	Thermal deformation temperature 0.45 MPa (°C)
PP	3.3	128
Fluorinated PP(PP20)	5.5	135

References

1. Kirsch P (2004) Modern Fluoroorganinc Chemistry-Synthesis, Reactivity, Applications [B]. Wiley, Hoboken, pp 8–9
2. Torres A (2007) Appl Surf Sci 254:1, doi:10.1016/j.apsusc.2007.07.122
3. Zhang Y, Tan K-L (2001) Langmuir 17:2265, doi:10.1021/la0013547
4. Toit FJD, Sanderson RD (1999) J Fluor Chem 98:107, doi:10.1016/S0022-1139(99)00091-3
5. Toit FJD, Sanderson RD (1999) J Fluor Chem 98:115, doi:10.1016/S0022-1139(99)00092-5
6. Kingsley KCH, Graham B, Shia G, Matalya V, Bismarck A (2007) J Fluor Chem 128:1359, doi:10.1016/j.jfluchem.2007.06.005
7. Dubois M, Guerin K, Giirandet J, Pilichowsko J-F, Thomas P, Delbe K et al (2005) Polym 46:6736, doi:10.1016/j.polymer.2005.06.029
8. Estelrich AR, Ameduri B (2004) Macromol Chem Phys 205:223, doi:10.1002/macp.200300014
9. Kassis CM, Steehler JK, Betts BE, Guan Z, Romack T, Joseph M (1996) Macromolecules 29:3247, doi:10.1021/ma951782x
10. Brown JR, Mathys Z (1997) J Mater Sci 32:2599, doi:10.1023/A:1018654501851
11. Bonfiovanni R, Gianni AD, Priola A, Pollicino A (2007) Eur Polym J 43:3787, doi:10.1016/j.eurpolymj.2007.06.037
12. Bongiovanni R, Gianni AD, Priola A, Pollicino A (2007) Eur Polym J 43:3787, doi:10.1016/j.eurpolymj.2007.06.037
13. Moad G (1999) 81 Prog Polym Sci 24:81, doi:10.1016/S0079-6700(98)00017-3
14. Russell KE (2002) Prog Polym Sci 27:1007, doi:10.1016/S0079-6700(02)00007-2
15. Ruggeri G, Aglietto M, Petragnani A, Ciardelli F (1983) Eur Polym J 19:863, doi:10.1016/0014-3057(83)90039-3
16. Huang H, Liu NC (1998) J Appl Polym Sci 67:1957, doi:10.1002/(SICI)1097-4628(19980321)67:12<1957::AID-APP1>3.0.CO;2-M
17. Oromehie AR, Hashemi SA, Meldrum IG, Waters DN (1997) Polym Int 42:117, doi:10.1002/(SICI)1097-0126(199701)42:1<117::AID-PI690>3.0.CO;2-N
18. Hong CK, Kim MJ, Oh SH, Lee YS, Nah C (2008) J Ind Eng Chem 14:236
19. Li Y, Xie XM, Guo B (2001) Polymer (Guildf) 42:3419, doi:10.1016/S0032-3861(00)00767-9
20. Owens DK, Wendt RC (1969) J Appl Polym Sci 13:1741, doi:10.1002/app.1969.070130815
21. Mo ZS, Zhang HF (2003) The structure of crystal polymer and the X-ray diffraction. Science, Beijing, pp 165–170
22. Yuan YP, Chen B, Zhang XQ (2007) Polym 48:5480, doi:10.1016/j.polymer.2007.07.025
23. Feng JC, Chen MC (2003) Polym Int 52:42, doi:10.1002/pi.984
24. Jacoby P (2007) Plast Addit Compounding 9:32, doi:10.1016/S1464-391X(07)70068-5
25. Li JX, Cheung WL (1999) Polymer (Guildf) 40:1219, doi:10.1016/S0032-3861(98)00345-0
26. Zhou JJ, Liu JG, Yan SK, Yan SK, Dong JY, Li L et al (2005) Polym 46:4077
27. Qing Y, Wei J (2004) Colloid Polym Sci 282:1236
28. Lezak E, Bartczak Z, Galeski A (2006) Polym 47:8562, doi:10.1016/j.polymer.2006.10.016
29. Dorina TH, Jozsef V, Gottfried WE, Julius Vancso G (2000) J Polym Sci. Part B Polym Phys 38:672, doi:10.1002/(SICI)1099-0488(20000301)38:5<672::AID-POLB4>3.0.CO;2-P